Energy range for quantum coherence

Filippo Giraldi*
School of Chemistry and Physics, University of KwaZulu-Natal
and National Institute for Theoretical Physics (NIThePP), KwaZulu-Natal,
Westville Campus, Durban 4000, South Africa
and Gruppo Nazionale per la Fisica Matematica (GNFM-INdAM)
c/o Istituto Nazionale di Alta Matematica Francesco Severi,
Citta' Universitaria, Piazza Aldo Moro 5, 00185 Roma, Italy
(Received 26 March 2015; published 11 June 2015)

Decoherence-free states have been found in Markovian open system dynamics and in the framework of non-Markovian fermionic environments. In the latter scenario we determine an energy range where quantum coherence is maintained over long times for every initial coherent configuration. In particular, for a two-state fermionic system interacting with a non-Markovian fermionic environment, undamped oscillating or stable coherence between the two energy eigenstates appears if the degenerate energy level is below a critical energy. If these energies coincide, the same behavior is observed in the superohmic regime and, under special conditions, the initial coherence is approached asymptotically. Equivalently, coherence persists if a defined dressed energy of the system is less than the band-gap energy of the reservoir. Same properties are found in the framework of bosonic environments.

DOI: 10.1103/PhysRevA.91.062112 PACS number(s): 03.65.Yz, 03.67.Pp

I. INTRODUCTION

Quantum coherence is the key ingredient for the realization of quantum information processing [1–4]. Consequently, the disruptive effects of the external environment on quantum coherence is one of the main obstacles to the development of quantum technologies [5]. Despite the action of the external environment the reduced dynamics can be unitary in a subspace of the Hilbert space of an open quantum system [2]. This subspace is decoherence free and its existence is related to the degeneracy of an eigenvalue of the interaction Hamiltonian [6]. Decoherence-free states are obtained in several ways, from symmetries of the Hamiltonian [7] and semigroup approach [8], both in the Markovian [9] and non-Markovian regime [10], to name a few. The experimental realizations of decoherence-free subspaces are the most various. Decoherence-free spaces have been found in neutron interferometry [11], nuclear spin dynamics [12], trapped ions [13], and polarization-entangled photons [14], to name a few. Especially, the engineering reservoir approach provides time-dependent decoherence-free evolution in the ground and excited states of an ion trapped in a dissipative cavity, or in a superconducting artificial atom coupled to a microwave cavity, to name a few [15].

If the open system dynamics is Markovian [16,17] the decoherence-free subspace [8] can be determined by evaluating the kernel of the decohering Gorini-Kossakowski-Sudarshan-Lindblad superoperator [18–20]. Since the open system can evolve outside the decoherence-free subspace [21] the condition for a global unitary Markovian open dynamics has also been determined by including the unitary Hamiltonian evolution [9].

Increasing interest has been devoted to the non-Markovian open system dynamics in fermionic environments [22–36]. This theoretical model can describe quantum dots and nanodevices embedded in a large variety of nanostructures that are suitable for the implementation of quantum information processing. The nonequilibrium transport theory and the Schwinger-Keldysh nonequilibrium Green's-function technique provide for the non-Markovian open dynamics master equations with time-local decoherence rates [22,37]. By considering a fermionic open system with two degenerate energy levels, the enlightening analysis performed in Ref. [38] shows the existence of dynamically stabilized decoherence-free pure states. Full quantum coherence persists in the nanosystem despite the effect of the fermionic environment.

As a continuation of the above scenario, we consider a two-level nanoelectronic system interacting with a fermionic environment. As a further way to protect quantum coherence, we search for conditions on the energy that may maintain coherence in the nanosystem.

The paper is organized as follows. Section II is devoted to the description of the model. In Sec. III coherence between the quantum states of the nanosystem is analyzed in terms of the spectral density of the fermionic reservoir and an energy range is identified where partial coherence is maintained. Inverse power-law relaxations to the asymptotic regimes are obtained for a class of sub- and superohmic spectral densities in Sec. IV. Special cases are considered in Sec. V and the corresponding open system dynamics is described in terms of special functions. In Sec. VI coherence in bosonic environment is analyzed. Section VII is devoted to the conclusions, and details on the calculations are provided in the Appendix.

II. MODEL

A general nanoelectronic system interacting with a fermionic reservoir is described by the Hamiltonian $H = H_S + H_R + H_I$, where H_S represents the Hamiltonian of the system, H_R is the Hamiltonian of the reservoir, and H_I

*giraldi.filippo@gmail.com

represents the interaction term [38],

$$H_S = \sum_{j=1}^{N} E_j a_j^\dagger a_j, \quad H_R = \sum_k \varepsilon_k c_k^\dagger c_k, \tag{1}$$

$$H_I = \sum_{j=1}^{N} \sum_k g_{j,k}(e^{\imath\phi_j} a_j^\dagger c_k + e^{-\imath\phi_j} c_k^\dagger a_j). \tag{2}$$

The energy levels of the system are $E_1, \ldots, E_N$, while the creation and the annihilation operators related to the jth energy level E_j are $a_j^\dagger$ and a_j, respectively. Similarly, the creation and annihilation operators of the kth energy level ε_k of the reservoir are $c_k^\dagger$ and c_k, respectively. The real coefficient $g_{j,k}$ and the phase ϕ_j define the coupling strength between the jth energy level of the nanosystem and the kth level of the reservoir. The imaginary unity is $\imath$ and $\hbar = 1$.

In the following, we consider a nanosystem with two degenerate energy levels, $N = 2$ and $E_1 = E_2 = E_0$, that are identically coupled to the fermionic reservoir, $g_{1,k} = g_{2,k} = 2^{-1/2} g_k$. Following Ref. [38], the open system dynamics is well described via the fermion operators A_+ and A_-,

$$A_+ = \frac{a_1 + e^{\imath(\phi_1 - \phi_2)} a_2}{2^{1/2}}, \quad A_- = \frac{a_2 - e^{\imath(\phi_2 - \phi_1)} a_1}{2^{1/2}}. \tag{3}$$

In this way, the system and the interaction Hamiltonian read

$$H_S = E_0(A_+^\dagger A_+ + A_-^\dagger A_-), \tag{4}$$

$$H_I = \sum_k g_k(e^{\imath\phi_1} A_+^\dagger c_k + e^{-\imath\phi_1} A_+ c_k^\dagger). \tag{5}$$

Furthermore, the states $|+\rangle$ and $|-\rangle$ are defined as coherent superpositions of the original energy eigenstates $|1\rangle$ and $|2\rangle$ of the nanosystem,

$$|+\rangle = 2^{-1/2}(|1\rangle + e^{-\imath\phi}|2\rangle), \tag{6}$$

$$|-\rangle = 2^{-1/2}(|2\rangle - e^{\imath\phi}|1\rangle), \tag{7}$$

while $|v\rangle$ and $|d\rangle$ represent the vacuum and the doubly occupied electron state. The following relationships hold on the basis: $\{|+\rangle, |-\rangle, |v\rangle, |d\rangle\}$, $A_+^\dagger|+\rangle = A_+|-\rangle = A_+|v\rangle = A_+^\dagger|d\rangle = 0$, $A_+|+\rangle = |v\rangle$, $A_+^\dagger|-\rangle = |d\rangle$, $A_+^\dagger|v\rangle = |+\rangle$, $A_+|d\rangle = A_-^\dagger|v\rangle = |-\rangle$, $|1\rangle = a_1^\dagger|v\rangle$, $|2\rangle = a_2^\dagger|v\rangle$. The vanishing commutator $[A_-^\dagger A_-, H]$ suggests that the open dynamics is closed in the subspaces $\{|+\rangle, |v\rangle\}$ and $\{|-\rangle, |d\rangle\}$ that correspond to the expectation value $\langle A_-^\dagger A_-\rangle$ of the occupation number equal to 0 and 1, respectively.

Following Refs. [25–33,38], the time evolution of this open system is described by the master equation

$$\dot{\rho}(t) = -\imath[H_S', \rho(t)] + L[\rho(t)], \tag{8}$$

where $\rho(t)$ represents the density matrix. The renormalized system Hamiltonian H_S' and the decohering superoperator L are defined in terms of the fermion operators A_+ and A_- as follows:

$$H_S' = E_r(t) A_+^\dagger A_+ + E_0 A_-^\dagger A_-, \tag{9}$$

$$L[\rho(t)] = k(t)[2A_+\rho(t)A_+^\dagger - A_+^\dagger A_+\rho(t) - \rho(t)A_+^\dagger A_+] + k_r(t)[2A_+^\dagger\rho(t)A_+ - A_+A_+^\dagger\rho(t) - \rho(t)A_+A_+^\dagger]. \tag{10}$$

The renormalized energy level $E_r(t)$ and the decoherence rates $k(t)$ and $k_r(t)$ are determined by the nonequilibrium retarded Green's functions $u(t)$ and nonequilibrium correlation Green's functions $u_c(t)$,

$$E_r(t) = -\mathrm{Im}\{\dot{u}(t)u^{-1}(t)\}, \tag{11}$$

$$k(t) = u_c(t)\mathrm{Re}\{\dot{u}(t)u^{-1}(t)\} - \mathrm{Re}\{\dot{u}(t)u^{-1}(t)\} - \dot{u}_c(t)/2, \tag{12}$$

$$k_r(t) = \dot{u}_c(t)/2 - u_c(t)\mathrm{Re}\{\dot{u}(t)u^{-1}(t)\}. \tag{13}$$

The Green's functions are provided by the Schwinger-Keldish formalism of nonequilibrium transport theory [37]. The retarded Green's function $u(t)$ is obtained as the solution of the following integrodifferential equation:

$$\dot{u}(t) + \imath E_0 u(t) + \int_0^t g(t - t')u(t')dt' = 0, \tag{14}$$

where

$$g(\tau) = \int_{\Omega_g}^{\infty} J(\omega)e^{-\imath\omega\tau}d\omega. \tag{15}$$

The function $J(\omega)$ represents the environmental spectral density, $J(\omega) = \sum_k |g_k|^2\delta(\omega - \omega_k)$, and Ω_g is the band-gap frequency of the reservoir. The correlation Green's function $u_c(t)$ is defined in terms of the retarded Green's function,

$$u_c(t) = \int_0^t dt' \int_0^t u(t')g_T(t'' - t')u^*(t'')dt'', \tag{16}$$

where

$$g_T(\tau) = \int_{\Omega_g}^{\infty} \frac{J(\omega)e^{-\imath\omega\tau}}{e^{(\omega-\mu_f)/(k_BT)} + 1} d\omega. \tag{17}$$

The parameter μ_f represents the external bias, k_B is the Boltzmann constant, and T is the absolute temperature. Finally, the exact solution of the master equation (8) is given by the following form [38]:

$$\rho(t) = \rho_{+,+}(t)|+\rangle\langle+| + \rho_{+,-}(t)|+\rangle\langle-| + \rho_{+,-}^*(t)|-\rangle\langle+| + \rho_{-,-}(t)|-\rangle\langle-| + \rho_{v,v}(t)|v\rangle\langle v| + \rho_{d,d}(t)|d\rangle\langle d|, \tag{18}$$

where

$$\rho_{+,+}(t) = \rho_{+,+}(0)[|u(t)|^2 + u_c(t)] + \rho_{v,v}(0)u_c(t), \tag{19}$$

$$\rho_{+,-}(t) = \rho_{+,-}(0)e^{\imath E_0 t}u(t), \tag{20}$$

$$\rho_{-,-}(t) = \rho_{-,-}(0)[1 - u_c(t)] + \rho_{d,d}(0)[1 - |u(t)|^2 - u_c(t)], \tag{21}$$

$$\rho_{v,v}(t) = \rho_{v,v}(0)[1 - u_c(t)] + \rho_{+,+}(0)[1 - |u(t)|^2 - u_c(t)], \tag{22}$$

$$\rho_{d,d}(t) = \rho_{-,-}(0)u_c(t) + \rho_{d,d}(0)[|u_c(t)|^2 + u_c(t)]. \tag{23}$$

Following Ref. [38], the physical decoherence-free states are obtained iff one of the two decoherence rates vanishes dynamically. Beside mixed states, the possible pure dynamically stabilized decoherence-free states of the present system are $|+\rangle, |-\rangle, |v\rangle, |d\rangle$.

III. ENERGY RANGE FOR COHERENCE

We search for conditions that maintain quantum coherence between the states $|+\rangle$ and $|-\rangle$ of the nanosystem that linearly interacts with a fermionic environment. In general, the open dynamics is characterized by three typical time scales [22]. The typical time scale of the nanosystem is $1/E_0$. The typical time scale of the environment is $1/\delta_\omega$, where δ_ω represents the bandwidth of the environmental spectral density. The interaction between system and environment provides a further time scale that is estimated by the inverse of the coupling strength. Here, the evolution of the coherence term is described by introducing a time scale $1/\omega_s$. The scale frequency ω_s arises from the environmental spectral density and scaling properties. In fact, the spectral density is defined via the auxiliary function $\Lambda(\nu)$ as $J(\omega+\Omega_g)=\Lambda(\nu)$, where $\nu=\omega/\omega_s$, for every $\omega \geqslant 0$. The physical conditions that maintain coherence will be determined by the interplay between the scale frequency ω_s and integral properties of the auxiliary function. Throughout the whole paper the regular spectral densities under study do not vanish above the band-gap frequency, $J(\omega)>0$ for every $\omega>\Omega_g$. The spectral densities are limited over the interval $[\Omega_g,+\infty)$ and summable, $J(\omega)\in L_1[\Omega_g,+\infty)$. The absence of any band gap in the reservoir is obviously included by setting $\Omega_g=0$.

If the two states are initially coherently coupled, i.e., $\rho_{+,-}(0)\neq 0$, persistence, undamped oscillations, or total loss of coherence are observed over long times. The appearance of each condition depends on a critical energy E_c that is determined by integral properties of the spectral density and the band-gap energy of the reservoir,

$$E_c=\Omega_g+\int_{\Omega_g}^{\infty}\frac{J(\omega)}{\omega-\Omega_g}\,d\omega. \tag{24}$$

If the degenerate energy level E_0 of the nanoelectric system is below the critical energy E_c of the reservoir, the coherence term results in

$$\rho_{+,-}(t)=\rho_{+,-}(0)\,e^{\imath(E_0-\Omega_g)t} \times[\gamma e^{\imath\Delta\omega_s t}+I(\omega_s t)],\quad E_0<E_c. \tag{25}$$

The coefficients γ and Δ are defined in the Appendix via the auxiliary function $\Lambda(\nu)$. The transient function $I(\omega_s t)$ is determined by the spectral density,

$$I(\omega_s t)=\int_{0^+}^{\infty}e^{-\imath\omega t}J(\omega+\Omega_g)/(\{\omega-E_0+\Omega_g+\mathcal{H}_+[J(\omega'+\Omega_g),\omega]\}^2+\pi^2J^2(\omega+\Omega_g))\,d\omega, \tag{26}$$

via the one-sided Hilbert transform, $\mathcal{H}_+[\varphi(\omega'),\omega]=\fint_0^\infty\varphi(\omega')/(\omega'-\omega)d\omega'$. The bar refers to the Cauchy principal value at $\omega'=\omega$. Over long times, $t\gg 1/\omega_s$, the transient function $I(\omega_s t)$ vanishes and undamped oscillations of the coherence term appear,

$$\rho_{+,-}(t)\sim\rho_{+,-}(0)\,e^{\imath(E_0-\Omega_g)t}\gamma e^{\imath\Delta\omega_s t},\quad E_0<E_c. \tag{27}$$

The frequency of the undamped oscillations is constant $\left(E_0-\Omega_g+\Delta\omega_s\right)$, and vanishes for a special value of the band-gap frequency, $\Omega_g=E_0+\Delta\omega_s$. In this case coherence persists for $t\gg 1/\omega_s$,

$$\rho_{+,-}(t)\sim\gamma\rho_{+,-}(0),\quad E_0<E_c,\quad \Omega_g=E_0+\Delta\omega_s. \tag{28}$$

The above analysis holds also if the critical energy is infinite, $E_c=+\infty$. This condition is due to the divergence of the improper integral appearing on the right-hand side of Eq. (24). For example, the critical energy is infinite for spectral densities that do not vanish in the band-gap frequency, $J(\Omega_g)>0$. On the contrary, the critical energy is finite for spectral densities that are super- or subohmic in the band-gap frequency, $J(\omega)\sim a_0(\omega-\Omega_g)^{\alpha_0}$ for $\omega\to\Omega_g^+$ with $\alpha_0>1$ or $1>\alpha_0>0$, respectively [39].

If the degenerate energy level of the nanoelectric system is equal to the critical energy of the reservoir, the appearance of persistence, undamped oscillations or total loss of coherence over long times is determined by the structure of the spectral density at low frequencies. For spectral densities that are superohmic in the band-gap frequency the coherence term results to be

$$\rho_{+,-}(t)=\rho_{+,-}(0)e^{\imath(E_0-\Omega_g)t}[\gamma_c+I_S(\omega_s t)],\quad E_0=E_c,\quad \alpha_0>1, \tag{29}$$

where

$$\gamma_c=\left(1+\frac{1}{\omega_s}\int_{\Omega_g}^{\infty}\frac{J(\omega)}{(\omega-\Omega_g)^2}\,d\omega\right)^{-1}. \tag{30}$$

The transient term $I_S(\omega_s t)$ is given by the following form:

$$I_S(\omega_s t)=\int_{0^+}^{\infty}\frac{J(\omega+\Omega_g)e^{-\imath\omega t}}{\omega^2}\Bigg/\left[\left(\frac{\pi J(\omega+\Omega_g)}{\omega}\right)^2+\left(1+\mathcal{H}_+\left[\frac{J(\omega'+\Omega_g)}{\omega'},\omega\right]\right)^2\right]d\omega \tag{31}$$

and vanishes over long times. Consequently, undamped oscillations of the coherence term appear for $t\gg 1/\omega_s$,

$$\rho_{+,-}(t)\sim\gamma_c\rho_{+,-}(0)e^{\imath(E_0-\Omega_g)t},\quad E_0=E_c,\quad \alpha_0>1, \tag{32}$$

and persistence of coherence is obtained in the same regime if the band-gap energy coincides with the energy level of the nanosystem,

$$\rho_{+,-}(t)\sim\gamma_c\rho_{+,-}(0),\quad E_0=E_c=\Omega_g,\quad \alpha_0>1. \tag{33}$$

Let the degenerate energy level of the nanoelectric system be equal to the critical energy of the reservoir. For subohmic spectral densities such that $J(\omega)\sim\sum_{j=0}^{\infty}a_j(\omega-\Omega_g)^{\alpha_j}$ for $\omega\to\Omega_g^+$, with $0<\alpha_0<1$ and $\alpha_j\neq 1$ for every $j=1,2,\ldots$, the coherence term is

$$\rho_{+,-}(t)=\rho_{+,-}(0)e^{\imath(E_0-\Omega_g)t}I(\omega_s t),\quad E_0=E_c,\quad 1>\alpha_0>0, \tag{34}$$

and vanishes for $t\gg 1/\omega_s$.

If the degenerate energy level of the nanoelectric system is above the critical energy of the reservoir the coherence term reads

$$\rho_{+,-}(t) = \rho_{+,-}(0)e^{\imath(E_0-\Omega_g)t} I(\omega_s t), \quad E_0 > E_c, \tag{35}$$

and vanishes for $t \gg 1/\omega_s$.

In summary, if the states $|+\rangle$ and $|-\rangle$ of the nanosystem are initially coherently coupled, i.e., $\rho_{+,-}(0) \neq 0$, undamped oscillations of the coherence term appear over long times, $t \gg 1/\omega_s$, under each of the two following conditions: the degenerate energy level of the nanosystem is lower than the critical energy, $E_0 < E_c$, or the degenerate energy level of the nanosystem is equal to the critical energy, $E_0 = E_c$, and the spectral density is superohmic, $\alpha_0 > 1$, in the band-gap frequency Ω_g. The oscillations disappear and coherence becomes persistent for special values of the band-gap frequency. The second condition, $E_0 = E_c$ and $\alpha_0 > 1$, is of interest for the protection and control of the initial coherence. In fact, over long times, $t \gg 1/\omega_s$, the magnitude of the coherence term approaches its initial value,

$$\rho_{+,-}(t) \sim \rho_{+,-}(0)e^{\imath(E_0-\Omega_g)t}, \tag{36}$$

for

$$\int_{\Omega_g}^{\infty} \frac{J(\omega)}{(\omega-\Omega_g)^2}\, d\omega \ll \omega_s, \quad E_0 = E_c, \quad \alpha_0 > 1. \tag{37}$$

Especially, if the conditions (37) hold and if $\Omega_g = E_0 = E_c$, the oscillations disappear and the coherence term approaches the initial value, $\rho_{+,-}(t) \sim \rho_{+,-}(0)$, over long times, $t \gg 1/\omega_s$. Qualitatively, the first of the conditions (37) can be obtained slightly above the ohmic regime, $\alpha_0 \gtrsim 1$, where the dominant low-frequency contribution to the integration is small, or if the scale frequency ω_s is adequately larger than the negative second moment of the auxiliary function of the spectral density.

The above analysis shows how coherence can be maintained in a degenerate two-level system interacting with a fermionic environment if the energy E_0 of the nanosystem is less than or, in the superohmic regime, equal to the critical energy E_c. This behavior exhibits analogies with the fractionalized steady-state inversion phenomena that appear in a two-level atom embedded in a photonic band-gap material [40–42]. In fact, the quantity $\int_{\Omega_g}^{\infty} J(\omega)/\left(\omega-\Omega_g\right)\, d\omega$, belonging to the expression of the critical energy E_c, can be interpreted as a negative energy shift in the energy E_0 of the nanosystem that is due to the interaction with the fermionic reservoir. In this way, the persistence of coherence can be explained via the mutual interplay between the band-gap energy Ω_g of the fermionic reservoir and the "dressed" energy E_d that is defined as follows:

$$E_d = E_0 - \int_{\Omega_g}^{\infty} \frac{J(\omega)}{\omega-\Omega_g}\, d\omega. \tag{38}$$

If the dressed energy is below the band-gap energy, $E_d < \Omega_g$, oscillating or stable coherence is maintained in the nanosystem over long times. If the dressed energy exceeds the band-gap energy, $E_d > \Omega_g$, coherence is entirely lost over long times. If the dressed energy equals the band-gap energy, $E_d = \Omega_g$, threshold effects appear and the loss of coherence depends on the structure of the environmental spectral density in the band-gap frequency. As reported above, coherence is completely lost in the subohmic regime and persists asymptotically in superohmic conditions.

IV. INVERSE POWER-LAW RELAXATIONS

The long-time behaviors of the coherence term $\rho_{+,-}(t)$ are determined by the decays of the transient functions $I(\omega_s t)$ and $I_S(\omega_s t)$. We intend to analyze the dependence of these decays on the low-frequency structure of the spectral density. Usually, the spectral densities are shaped as power laws at low frequencies with an exponential cutoff at high frequencies [3,38]. Here, we consider a class of spectral densities with a band gap that are super- or subohmic in the band-gap frequency. For the sake of simplicity, this class is defined by imposing certain constraints over the auxiliary function $\Lambda(\nu)$ introduced in the previous section. The constraint concerning the low-frequency behavior is the following:

$$\Lambda(\nu) \sim \sum_{n=0}^{\infty} a_n \nu^{\alpha_n}, \quad \nu \to 0^+, \tag{39}$$

where $\alpha_0 > 0$, $\alpha_{n+1} > \alpha_n$ and $\alpha_n \neq \lfloor \alpha_n \rfloor$ for every natural value of the index n. The functions $\Lambda(\nu)$ are regular and continuously differentiable $(\lfloor \alpha_0 \rfloor + 2)$ times, at least, in $(0,\infty)$. The spectral densities are shaped quite arbitrarily at high frequencies by requiring the physical constraints of summability, $\sup\{\delta \mid \Lambda(\nu) = O(\nu^{-1-\delta}), \nu \to +\infty\} > 0$, and the convergence of the integral $\int_1^{\infty} |\Lambda^{(l)}(\nu)| d\nu$ for every $l = 0, 1, \ldots, \lfloor \alpha_0 \rfloor + 2$.

In the following, we analyze the behavior of the coherence terms that are induced by the above class of spectral densities. If the degenerate energy level of the nanoelectric system is below the critical energy of the reservoir the transient term $I(\omega_s t)$ exhibits inverse power-law decays that are arbitrarily faster than $1/(\omega_s t)$. The resulting coherence term behaves for $t \gg 1/\omega_s$ as follows:

$$\rho_{+,-}(t) \sim \rho_{+,-}(0)e^{\imath(E_0-\Omega_g)t}[\gamma e^{\imath \Delta\omega_s t} + \eta(\omega_s t)^{-1-\alpha_0}], \quad E_0 < E_c. \tag{40}$$

The coefficient η is defined in the Appendix.

If the degenerate energy level of the nanoelectric system is equal to the critical energy of the reservoir, if the spectral density belongs to the above class and is superohmic in the band-gap frequency, the transient term $I_S(\omega_s t)$ exhibits long-time arbitrarily slow inverse power-law decays. Consequently, for $t \gg 1/\omega_s$ the resulting coherence term reads

$$\rho_{+,-}(t) \sim \rho_{+,-}(0)e^{\imath(E_0-\Omega_g)t}[\gamma_c + \eta_c(\omega_s t)^{1-\alpha_0}], \quad E_0 = E_c, \quad \alpha_0 > 1. \tag{41}$$

The coefficient η_c is defined in the Appendix.

If the degenerate energy level of the nanoelectric system is equal to the critical energy of the reservoir and the spectral density belongs to the above class and is subohmic in the band-gap frequency, the transient term $I(\omega_s t)$ decays over long times according to arbitrarily slow inverse power laws. The resulting coherence term is described for $t \gg 1/\omega_s$ by the following form:

$$\rho_{+,-}(t) \sim \eta_s \rho_{+,-}(0)e^{\imath(E_0-\Omega_g)t}(\omega_s t)^{\alpha_0-1}, \quad E_0 = E_c, \quad 1 > \alpha_0 > 0. \tag{42}$$

The coefficient η_s is defined in the Appendix.

If the degenerate energy level of the nanoelectric system is above the critical energy of the reservoir and the spectral density belongs to the above class, the transient term $I(\omega_s t)$ results over long times in inverse power-law decays. These relaxations are arbitrarily faster than $1/(\omega_s t)$ and for $t \gg 1/\omega_s$ the coherence term reads

$$\rho_{+,-}(t) \sim \eta \rho_{+,-}(0) e^{\imath (E_0 - \Omega_g)t} (\omega_s t)^{-1-\alpha_0}, \quad E_0 > E_c. \tag{43}$$

In occurrence of the resonance $E_0 = E_c$ the relaxations to the asymptotic configurations become arbitrarily slow by approaching the boundary between sub- and superohmic regime, i.e., $\alpha_0 \to 1^-$ in the subohmic regime and $\alpha_0 \to 1^+$ in the superohmic condition. This behavior has been found in the general non-Markovian open system dynamics of finite dimensional open quantum systems in bosonic environments [43].

V. SPECIAL CASES

We study the quantum coherence that exists between the two states $|+\rangle$ and $|-\rangle$ of the nanosystem by considering two special forms of spectral densities. The spectral density $J_1(\omega)$ is defined by the following expression:

$$J_1(\omega) = \frac{j_1 \left(\frac{\omega - \Omega_g}{\omega_s}\right)^{\alpha}}{\lambda^2 + \left(\frac{\omega - \Omega_g}{\omega_s}\right)^2}, \quad 1 > \alpha > 0, \tag{44}$$

and is subohmic in the band-gap frequency. The spectral density $J_2(\omega)$ is defined as follows:

$$J_2(\omega) = \frac{j_2 \left(\frac{\omega - \Omega_g}{\omega_s}\right)^{\beta}}{\left(l + \frac{\omega - \Omega_g}{\omega_s}\right)\left[\lambda^2 + \left(\frac{\omega - \Omega_g}{\omega_s}\right)^2\right]}, \tag{45}$$

for $2 > \beta > 0$, it is superohmic in the band-gap frequency for $2 > \beta > 1$ and subohmic for $1 > \beta > 0$. The parameters j_1 and j_2 depend on the coupling between open system and environment and on the reservoir correlation time [2].

The time evolution of the coherence term is described in terms of the Fox H-function [44]. This special function is defined by the following expression:

$$H_{p,q}^{m,n}\left[z \middle| \begin{matrix}(a_1, A_1), \ldots, (a_p, A_p) \\ (b_1, B_1), \ldots, (b_q, B_q)\end{matrix}\right] = \frac{1}{2\pi\imath} \int_{\mathcal{C}} \frac{\Pi_{j=1}^{m} \Gamma(b_j + B_j s) \Pi_{j=1}^{n} \Gamma(1 - a_j - A_j s) z^{-s}}{\Pi_{j=m+1}^{q} \Gamma(1 - b_j - B_j s) \Pi_{j=n+1}^{p} \Gamma(a_j + A_j s)}\, ds,$$

under the conditions that the poles of the Γ functions, appearing in the denominator, do not coincide. The empty products are interpreted as unity. The natural numbers m,n,p,q fulfill the following constraints: $0 \leqslant n \leqslant p$, $1 \leqslant m \leqslant q$, $A_j, B_k \in (0, +\infty)$, for every $j = 1, \ldots, p$ and $k = 1, \ldots, q$. For the sake of shortness, we refer to [44] for details on the contour path $\mathcal{C}$, the existence, and the properties of the Fox H-function. If the environmental spectral density is described by the form $J_1(\omega)$ the coherence term results in

$$\begin{aligned}\rho_{+,-}(t) = \rho_{+,-}(0) e^{\imath (E_0 - \Omega_g)t} \sum_{n=0}^{\infty} \sum_{k=0}^{n} \sum_{j=0}^{k} C_{n,k,j}^{(1)} (\omega_s t)^{2n+k-\alpha j} \\ \times \left(H_{1,2}^{1,1}\left[\imath r_2 \omega_s t \middle| \begin{matrix}(-n,1) \\ (0,1), (-2n-k+\alpha j, 1)\end{matrix}\right] - (\lambda \omega_s t)^2 H_{1,2}^{1,1}\left[\imath r_2 \omega_s t \middle| \begin{matrix}(-n,1) \\ (0,1), (-2n-k+\alpha j - 2, 1)\end{matrix}\right]\right).\end{aligned} \tag{46}$$

If the environmental spectral density is described by the form $J_2(\omega)$ the coherence term reads

$$\begin{aligned}\rho_{+,-}(t) = \rho_{+,-}(0) e^{\imath (E_0 - \Omega_g)t} \sum_{n=0}^{\infty} \sum_{k=0}^{n} \sum_{j=0}^{k} \sum_{m=0}^{j} C_{n,k,j,m}^{(2)} (\omega_s t)^{2n+k+j-\beta m} \left(H_{1,2}^{1,1}\left[\imath q_3 \omega_s t \middle| \begin{matrix}(-n,1) \\ (0,1), (-2n-k-j+\beta m, 1)\end{matrix}\right] \right. \\ - \imath l \omega_s t H_{1,2}^{1,1}\left[\imath q_3 \omega_s t \middle| \begin{matrix}(-n,1) \\ (0,1), (-2n-k-j+\beta m - 1, 1)\end{matrix}\right] \\ - \lambda^2 (\omega_s t)^2 H_{1,2}^{1,1}\left[\imath q_3 \omega_s t \middle| \begin{matrix}(-n,1) \\ (0,1), (-2n-k-j+\beta m - 2, 1)\end{matrix}\right] \\ \left. + \imath l \lambda^2 (\omega_s t)^3 H_{1,2}^{1,1}\left[\imath q_3 \omega_s t \middle| \begin{matrix}(-n,1) \\ (0,1), (-2n-k-j+\beta m - 3, 1)\end{matrix}\right]\right).\end{aligned} \tag{47}$$

The coefficients $C_{n,k,j}^{(1)}$ and $C_{n,k,j,m}^{(2)}$ are defined in the Appendix. Since the spectral densities $J_1(\omega)$ and $J_2(\omega)$ belong to the general class defined in the previous section, the long-time behaviors are included in the cases reported above. The corresponding critical energies $E_{c,1}$ and $E_{c,2}$ read

$$E_{c,1} = \Omega_g + \frac{\pi}{2} j_1 \lambda^{\alpha - 2} \csc\left(\frac{\pi \alpha}{2}\right), \tag{48}$$

$$E_{c,2} = \Omega_g + \frac{\pi}{2(l^2 + \lambda^2)}\left[2 l^{\beta - 1} \csc(\pi\beta) + l \lambda^{\beta - 2} \csc\left(\frac{\pi\beta}{2}\right) - \lambda^{\beta - 1} \sec\left(\frac{\pi\beta}{2}\right)\right]. \tag{49}$$

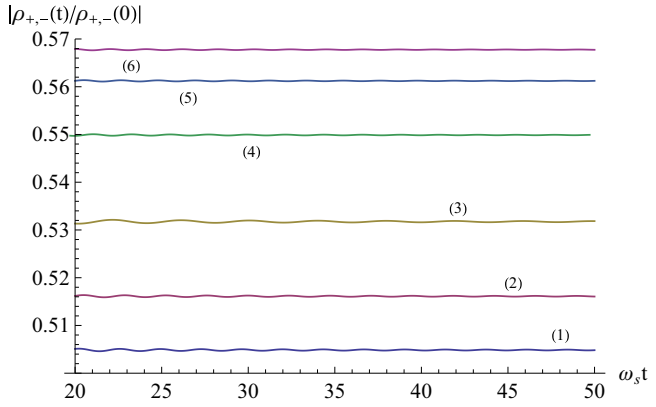

FIG. 1. (Color online) The ratio $|\rho_{+,-}(t)/\rho_{+,-}(0)|$ vs $(\omega_s t)$ for different values of $\rho_0 = (E_0 - \Omega_g)/\omega_s$, $\rho_c = (E_c - \Omega_g)/\omega_s$, α, $\rho_1 = j_1/\omega_s$, λ. Curve (1) corresponds to the values $\rho_0 = \lambda = 1$, $\rho_c \simeq 50.83$, $\alpha = 1/5$, $\rho_1 = 10$; curve (2) corresponds to $\rho_0 = \lambda = 1$, $\rho_c = 10\pi$, $\alpha = 1/3$, $\rho_1 = 10$; curve (3) corresponds to $\rho_0 = \lambda = 1$, $\rho_c \simeq 9.71$, $\alpha = 3/5$, $\rho_1 = 5$; curve (4) corresponds to $\rho_0 = \lambda = 1$, $\rho_c = 3^{-1/2}10\pi$, $\alpha = 2/3$, $\rho_1 = 10$; curve (5) corresponds to $\rho_0 = \lambda = 1$, $\rho_c = 5\pi \sec(\pi/8)$, $\alpha = 3/4$, $\rho_1 = 10$; curve (6) corresponds to $\rho_0 = \lambda = 1$, $\rho_c \simeq 16.52$, $\alpha = 4/5$, $\rho_1 = 10$. Each curve shows persistence of quantum coherence over long times.

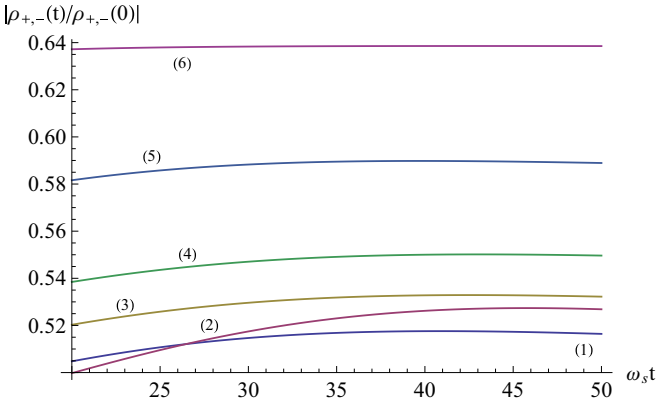

FIG. 2. (Color online) The ratio $|\rho_{+,-}(t)/\rho_{+,-}(0)|$ vs $(\omega_s t)$ for different values of the parameters ρ_0, ρ_c, β, ρ_2, λ, l. Curve (1) corresponds to the values $\rho_0 = 1/2$, $\rho_c \simeq 0.71$, $\beta = 7/6$, $\rho_2 = \lambda = l = 1$; curve (2) corresponds to $\rho_0 = 1/2$, $\rho_c \simeq 0.70$, $\beta = 6/5$, $\rho_2 = \lambda = l = 1$; curve (3) corresponds to $\rho_0 = 1/2$, $\rho_c \simeq 0.68$, $\beta = 5/4$, $\rho_2 = \lambda = l = 1$; curve (4) corresponds to $\rho_0 = 1/2$, $\rho_c \simeq 0.66$, $\beta = 4/3$, $\rho_2 = \lambda = l = 1$; curve (5) corresponds to $\rho_0 = 1/2$, $\rho_c \simeq 0.65$, $\beta = 3/2$, $\rho_2 = \lambda = l = 1$; curve (6) corresponds to $\rho_0 = 3/2$, $\rho_c = \pi/2$, $\beta = 5/2$, $\rho_2 = \lambda = l = 1$. Each curve shows persistence of quantum coherence over long times.

Simplified forms are obtained if the powers α and β take rational values p/q. In this cases the coherence term results in a finite sum,

$$\rho_{+,-}(t) = \rho_{+,-}(0)e^{\imath(E_0-\Omega_g)t}\sum_{l=1}^{n_j}\sum_{k=1}^{m_l^{(j)}}\Phi_{l,k}^{(j)}(\omega_s t)^{(m_l-k+1-q)/q} \times H_{1,2}^{1,1}\left[-\sigma_l^{(j)}(\omega_s t)^{1/q}\middle|\begin{matrix}(k-m_l^{(j)},1)\\(0,1),\left(\frac{q-m_l^{(j)}+k-1}{q},\frac{1}{q}\right)\end{matrix}\right], \quad (50)$$

where $j = 1,2$. The case $j = 1$ refers to the spectral density $J_1(\omega)$ and $j = 2$ to $J_2(\omega)$. The involved parameters n_j, $m_l^{(j)}$, $\sigma_l^{(j)}$, $\Phi_{l,k}^{(j)}$, are defined in the Appendix.

The numerical analysis shows long-time persistence of coherence in the condition $E_0 < E_c$ and in the superohmic regime of the resonance $E_0 = E_c$, in accordance with the theoretical analysis performed in the previous section. See Figs. 1 and 2. Furthermore, the inverse power-law decays of the coherence term are confirmed by the asymptotic lines appearing in the log-log plots of Figs. 3 and 4. Each slope coincides with the power of the inverse power-aw decay that is theoretically predicted in the previous section.

VI. BOSONIC ENVIRONMENT

The Feynman-Vernon influence functional approach in the coherent states representation provides an efficient way to describe the open dynamics of a nanodevice [45]. For a quantum dot coupled to a fermionic environment the master equation of the reduced density matrix is given by the following expression:

$$\dot{\rho}(t) = -\imath[H'(t),\rho(t)] + \gamma_e(t)[2a\rho(t)a^\dagger - \rho(t)a^\dagger a - a^\dagger a\rho(t)] + \tilde{\gamma}_e(t)[a\rho(t)a^\dagger + a^\dagger\rho(t)a - a^\dagger a\rho(t) - \rho(t)a^\dagger a], \quad (51)$$

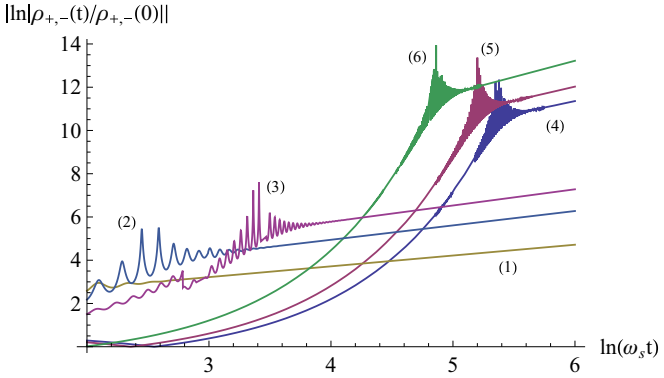

FIG. 3. (Color online) The quantity $|\ln|\rho_{+,-}(t)/\rho_{+,-}(0)||$ vs $\ln(\omega_s t)$ for different values of the parameters $\rho_0, \rho_c, \alpha, \rho_1, \lambda$. Curve (1) corresponds to the values $\rho_0 = \rho_c = 2^{-1/2}\pi$, $\alpha = 1/2$, $\rho_1 = \lambda = 1$; curve (2) corresponds to $\rho_0 = 10$, $\rho_c = \pi$, $\alpha = 1/3$, $\rho_1 = \lambda = 1$; curve (3) corresponds to $\rho_0 = \rho_c = \pi \csc(\pi/8)/2$, $\alpha = 1/4$, $\rho_1 = \lambda = 1$; curve (4) corresponds to $\rho_0 = 10$, $\rho_c = \pi \csc(\pi/8)/2$, $\alpha = 1/4$, $\rho_1 = \lambda = 1$; curve (5) corresponds to $\rho_0 = 10$, $\rho_c = \pi$, $\alpha = 1/3$, $\rho_1 = \lambda = 1$; curve (6) corresponds to $\rho_0 = 10$, $\rho_c = 2^{-1/2}\pi$, $\alpha = 1/2, \rho_1 = \lambda = 1$. For each curve the asymptotic line corresponds to the inverse power-law decay of the coherence term and the slope coincides with the theoretically predicted power.

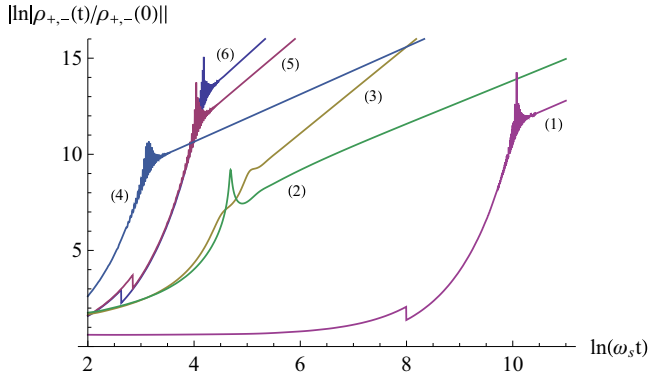

FIG. 4. (Color online) The quantity $|\ln|\rho_{+,-}(t)/\rho_{+,-}(0)||$ vs $\ln(\omega_s t)$ for different values of the parameters ρ_0, ρ_c, β, ρ_2, λ, l. Curve (1) corresponds to $\rho_0=\rho_2=\lambda=l=1$, $\rho_c\simeq 0.96$, $\beta=11/5$; curve (2) corresponds to $\rho_0=\rho_2=\lambda=l=1$, $\rho_c\simeq 0.71$, $\beta=7/6$; curve (3) corresponds to $\rho_0=\rho_2=\lambda=l=1$, $\rho_c\simeq 0.68$, $\beta=5/4$; curve (4) corresponds to $\rho_0=10$, $\rho_c\simeq 0.96$, $\rho_2=\lambda=l=1$, $\beta=11/5$; curve (5) corresponds to $\rho_0=4$, $\rho_c\simeq 0.66$, $\beta=4/3$ $\rho_2=\lambda=l=1$; curve (6) corresponds to $\rho_0=5$, $\rho_c\simeq 0.65$, $\beta=3/2$, $\rho_2=\lambda=l=1$. For each curve the asymptotic line witnesses the appearance of the inverse power-law decay of the coherence term and the slope coincides with the theoretically predicted power.

where $a^\dagger$ and a are the creation and annihilation operator, respectively. See Refs. [22,25–33,38] for details. The renormalized Hamiltonian $H'(t)$ reads $H'(t)=-\mathrm{Im}\{\dot{u}(t)u^{-1}(t)\}a^\dagger a$. The master equation (51) is time local and the two nonunitary terms drive the dissipation and fluctuation process. The dissipation coefficient is $\gamma_e(t)=-\mathrm{Re}\{\dot{u}(t)u^{-1}(t)\}$, while the fluctuation coefficient reads $\tilde{\gamma}_e(t)=\dot{u}_c(t)-2u_c(t)\mathrm{Re}\{\dot{u}(t)u^{-1}(t)\}$. The functions $u(t)$ and $u_c(t)$ are the nonequilibrium retarded and correlation Green's function of the system, respectively, and are defined in Sec. III via Eqs. (14) and (16). Following Ref. [31], the reduced dynamics of a nanocavity that is embedded in photonic crystals is also described by the master equation (51). In this case the creation and annihilation operators fulfill the bosonic commutation rule. This theoretical construct has been generalized to systems of noninteracting bosons (fermions), consisting of N single-particle energy levels, that are coupled to different bosonic (fermionic) reservoirs [22]. Following Refs. [22,31], every feature of the open dynamics is determined by the retarded and correlation Green's functions of the system. Especially, the nonvanishing asymptotic behavior of the retarded Green's function provokes a suppression of the decoherence process [31]. Section III is devoted to the constraints on the energy that guarantee nonvanishing long-time behavior of coherence or, equivalently, of the retarded Green's function. These conditions hold also for a bosonic system with one single-particle energy level E_0 that interacts with a bosonic environment. Consequently, coherence persists in this bosonic open system if $E_0<E_c$ or in the superohmic regime of the resonance $E_0=E_c$. Obviously, the critical energy E_c is defined by Eq. (24) with the bosonic environmental spectral density.

In the following we consider the decoherence process of a two-state system (qubit), $|0\rangle$ and $|1\rangle$, that interacts with a reservoir of bosonic modes under the rotating wave approximation [2,46–48]. By choosing $\hbar=1$, the Hamiltonian of the whole system is $H_Q+H_B+H_{QB}$, where

$$H_Q=\omega_0\,\sigma_+\sigma_-,\quad H_B=\sum_{k=1}^{\infty}\omega_k\,b_k^\dagger b_k, \tag{52}$$

$$H_{QB}=\sum_{k=1}^{\infty}\left[g_k^{(b)}\,\sigma_+ b_k+\left(g_k^{(b)}\right)^*\sigma_- b_k^\dagger\right]. \tag{53}$$

The rising and lowering operators, σ_+ and σ_-, respectively, act on the Hilbert space of the qubit and are defined as follows: $\sigma_+=\sigma_-^\dagger=|1\rangle\langle 0|$, while $b_k^\dagger$ and b_k represent the creation and annihilation operators acting on the Hilbert space of the kth bosonic mode. The coupling between the transition $|0\rangle\leftrightarrow|1\rangle$ and the kth bosonic mode is represented by the constant $g_k^{(b)}$, while ω_0 is the qubit transition frequency. If the qubit is initially unentangled from the vacuum state $|0\rangle_B$ of the bosonic reservoir,

$$|\Psi(0)\rangle=[c_0|0\rangle+c_1(0)|1\rangle]\otimes|0\rangle_B, \tag{54}$$

the density matrix of the qubit evolves as follows [2,48]:

$$\rho_{1,1}(t)=1-\rho_{0,0}(t)=\rho_{1,1}(0)\,|G(t)|^2, \tag{55}$$

$$\rho_{1,0}(t)=\rho_{0,1}^*(t)=\rho_{1,0}(0)\,e^{-\imath\omega_0 t}G(t). \tag{56}$$

The function $G(t)$ is the solution of the convolution equation

$$\dot{G}(t)+\int_0^t f(t-t')G(t')dt'=0, \tag{57}$$

where the initial condition is $G(0)=1$, while $f(\tau)$ is the correlation function,

$$f(\tau)=\int_0^\infty J(\omega)e^{-\imath(\omega-\omega_0)\tau}d\omega,$$

and $J(\omega)$ is the spectral density of the bosonic reservoir [2,48].

Similarly to the scenario of the fermionic environment, the persistence or undamped oscillations of coherence depends on a critical frequency ω_c that is determined by the spectral density and the band-gap frequency Ω_g of the bosonic reservoir,

$$\omega_c=\Omega_g+\int_{\Omega_g}^\infty\frac{J(\omega)}{\omega-\Omega_g}\,d\omega. \tag{58}$$

If the transition frequency of the qubit is less than the critical frequency the coherence term results in

$$\rho_{1,0}(t)=\rho_{1,0}(0)e^{-\imath\Omega_g t}[\gamma_b e^{\imath\Delta_b\omega_s t}+I(\omega_s t)],\quad \omega_0<\omega_c. \tag{59}$$

The coefficients γ_b and Δ_b are defined in the Appendix in terms of the auxiliary function $\Lambda(\nu)$ introduced in Sec. III. The transient function $I(\omega_s t)$ refers to the expression (26) where $J(\omega)$ is the spectral density of the bosonic environment. The transient function vanishes over long times and undamped oscillations of the coherence term appear

for $t \gg 1/\omega_s$,

$$\rho_{1,0}(t) \sim \gamma_b \rho_{1,0}(0) e^{\imath(\Delta_b\omega_s - \Omega_g)t}, \quad \omega_0 < \omega_c. \tag{60}$$

Especially, if the band-gap frequency coincides with the value $\Delta_b\omega_s$ stable persistence of coherence is obtained for $t \gg 1/\omega_s$,

$$\rho_{1,0}(t) \sim \gamma_b \rho_{1,0}(0), \quad \omega_0 < \omega_c, \quad \Omega_g = \Delta_b\omega_s.$$

The above features of the reduced dynamics holds also if the critical frequency is infinite, $\omega_c = +\infty$.

If the transition frequency of the qubit is equal to the critical frequency the appearance of persistence, undamped oscillations, or total loss of coherence over long times is again determined by the structure of the spectral density at low frequencies. For bosonic spectral densities that are superohmic in the band-gap frequency the coherence term results in

$$\rho_{1,0}(t) = \rho_{1,0}(0) e^{-\imath\Omega_g t} \left[\gamma_c + I_S(\omega_s t)\right], \quad \omega_0 = \omega_c, \quad \alpha_0 > 1. \tag{61}$$

The transient term $I_S(\omega_s t)$ is given by the expression (31), where $J(\omega)$ is the spectral density of the bosonic reservoir, and vanishes over long times. Consequently, the coherence term exhibits undamped oscillations for $t \gg 1/\omega_s$,

$$\rho_{1,0}(t) = \gamma_c \rho_{1,0}(0) e^{-\imath\Omega_g t}, \quad \omega_0 = \omega_c, \quad \alpha_0 > 1. \tag{62}$$

The frequency of the oscillations coincides with the band-gap frequency and vanishes for $\Omega_g = 0$. In this case coherence persists over long times, $t \gg 1/\omega_s$,

$$\rho_{1,0}(\infty) \sim \gamma_c \rho_{1,0}(0), \quad \omega_0 = \omega_c, \quad \Omega_g = 0, \quad \alpha_0 > 1. \tag{63}$$

If the transition frequency of the qubit is equal to the critical energy of the reservoir and the spectral density is subohmic in the band-gap frequency the coherence term results in

$$\rho_{1,0}(t) = \rho_{1,0}(0) e^{-\imath\Omega_g t} I(\omega_s t), \quad \omega_0 = \omega_c, \quad 1 > \alpha_0 > 0, \tag{64}$$

and vanishes over long times, $t \gg 1/\omega_s$. If the transition frequency of the qubit exceeds the critical frequency the coherence term reads

$$\rho_{1,0}(t) = \rho_{1,0}(0) e^{-\imath\Omega_g t} I(\omega_s t), \tag{65}$$

and vanishes for $t \gg 1/\omega_s$. Similarly to the decoherence process in fermionic environment, a "dressed" energy ϵ_d can be defined

$$\epsilon_d = \omega_0 - \int_{\Omega_g}^{\infty} \frac{J(\omega)}{\omega - \Omega_g}\, d\omega, \tag{66}$$

such that oscillating or stable coherence persists in the two-level system over long times if the dressed energy is below the band-gap energy, $\epsilon_d < \Omega_g$. Coherence is entirely lost if the dressed energy exceeds the band-gap energy, $\epsilon_d > \Omega_g$. The loss of coherence depends on the structure of the environmental spectral density in the band-gap frequency if the dressed energy equals the band-gap energy, $\epsilon_d = \Omega_g$. In fact, coherence is completely lost in the subohmic regime and persists over long times in superohmic environments.

By considering bosonic spectral densities that belong to the general class defined in Sec. IV, $J(\omega + \Omega_g) = \Lambda(\nu)$, the coherence term exhibits inverse power-law relaxations to the asymptotic regimes. If the transition frequency of the qubit is less or greater than the critical frequency the long-time relaxations to the oscillating regime are described by inverse power laws that are arbitrarily faster than $1/(\omega_s t)$,

$$\rho_{1,0}(t) \sim \rho_{1,0}(0) e^{-\imath\Omega_g t} [\gamma_b e^{\imath\Delta_b\omega_s t} + \eta_b (\omega_s t)^{-1-\alpha_0}], \quad \omega_0 < \omega_c, \tag{67}$$

$$\rho_{+,-}(t) \sim \rho_{+,-}(0) \eta_b e^{-\imath\Omega_g t} (\omega_s t)^{-1-\alpha_0}, \quad \omega_0 > \omega_c. \tag{68}$$

The coefficient η_b is defined in the Appendix. If the transition frequency of the qubit is equal to the critical frequency the long-time relaxations to the oscillating regime are described by arbitrarily slow inverse power laws,

$$\rho_{1,0}(t) \sim \rho_{1,0}(0) e^{-\imath\Omega_g t} [\gamma_c + \eta_c (\omega_s t)^{1-\alpha_0}], \quad \omega_0 = \omega_c, \quad \alpha_0 > 1, \tag{69}$$

$$\rho_{1,0}(t) \sim \eta_s \rho_{1,0}(0) e^{-\imath\Omega_g t} (\omega_s t)^{\alpha_0 - 1}, \quad \omega_0 = \omega_c, \quad 1 > \alpha_0 > 0. \tag{70}$$

The present analysis of the general evolution and long-time persistence of coherence improves the description of the open dynamics performed in Ref. [49].

By dropping the rotating wave approximation a referential model of a two-level system coupled to a bosonic environment is the so-called spin-boson model. This system has been widely studied with the most various approaches and the related literature is vast [3,50–60]. In Ref. [61] a relevant and detailed analysis of the spin-boson model shows that an increase of the coupling strength between the system and the bosonic environment hinders the decoherence process via a transition from vanishing relaxations to lossless oscillations. Persistence of coherence has been also observed at vanishing temperatures [62] and, recently, under certain approximations, in the delocalized phase regime of the spin-boson model [63] by considering the spectral density (44). In the latter scenario we intend to generalize the conditions that protect coherence via the approach adopted in Sec. III.

The Hamiltonian of the spin-boson model is

$$H_{SB} = \frac{\epsilon}{2}\sigma_3 - \frac{\Omega}{2}\sigma_1 + \sum_k \frac{g_{b,k}}{2}\sigma_3(b_k + b_k^\dagger) + \sum_k \omega_k b_k^\dagger b_k, \tag{71}$$

where the sums are performed over the bosonic modes of the reservoir. The parameters ϵ and Ω refer to the energy difference and the transition amplitude between the two levels, respectively, and $\hbar = 1$. The Pauli operators σ_1, σ_2, σ_3, act on the Hilbert space of the two-level system. Following Ref. [61], the unitary transformation $U_1 = \exp\{-\imath\pi\sigma_2/4\}$ and the successive rotating wave approximation leads, for vanishing ϵ, to the following exactly solvable Hamiltonian:

$$H_{RWA} = \frac{\Omega}{2}\sigma_3 + \sum_k \frac{g_{b,k}}{2}(\sigma_+ b_k + \sigma_- b_k^\dagger) + \sum_k \omega_k b_k^\dagger b_k. \tag{72}$$

The initial condition is $|\Psi(0)\rangle = |+\rangle \otimes |0\rangle_B$, and corresponds to $|\Psi_1(0)\rangle = U_1|\Psi(0)\rangle = |+\rangle_1 \otimes |0\rangle_B$ in the rotated frame.

The time evolution [61] is

$$|\Psi_1(t)\rangle = e^{\imath\Omega t/2}\left(2^{-1/2}|-\rangle\otimes|0\rangle_B + c(t)|+\rangle\otimes|0\rangle_B + \sum_k d_k(t)|-\rangle\otimes|1_k\rangle_E\right), \tag{73}$$

where $|1_k\rangle_B = b_k^\dagger|0\rangle_B$ for every $k = 1,2,\ldots$, and $\sigma_1|\pm\rangle_x = \pm|\pm\rangle_x$. The coherence between the two levels is analyzed via the expectation value of the operator σ_1. This value corresponds to the polarization $\langle\Psi(t)|\sigma_3|\Psi(t)\rangle$ in the original frame, which means $P_z(t) = \langle\Psi_1(t)|\sigma_1|\Psi_1(t)\rangle$. For this reason the subindex z is chosen. Starting from the initial value $P_z(0) = 1$, under the rotating wave approximation, the polarization reads

$$P_z(t) = 2^{1/2}\mathrm{Re}\{c(t)\}, \tag{74}$$

where the function $c(t)$ is the solution of the following convoluted equation:

$$\dot{c}(t) + \imath\Omega c(t) + \int_0^t f_b\left(t-t'\right)c(t')dt' = 0, \tag{75}$$

where the initial condition is $c(0) = 2^{-1/2}$, while f_b denotes the correlation function of the reservoir.

Various perturbation approaches to the spin-boson model are based on unitary transformations [59–61]. Consider the transformed Hamiltonian H'_{SB} that is obtained from the Hamiltonian (71) via the unitary transformations U_1 and $U_2 = \exp\{\sum_k \varphi_k g_{b,k}\sigma_1(b_k^\dagger - b_k)/(2\omega_k)\}$. The resulting Hamiltonian is $H'_{SB} = H'_0 + H'_1 + H'_2$, where

$$H'_0 = \frac{\theta\Omega}{2}\sigma_3 + \sum_k \omega_k b_k^\dagger b_k + C_0, \tag{76}$$

$$H'_1 = \sum_k g'_k\left(\sigma_+ b_k + \sigma_- b_k^\dagger\right), \tag{77}$$

$$H'_2 = \frac{\Omega}{2}\sigma_3(\cosh\chi - \theta) - \imath\frac{\Omega}{2}\sigma_2(\sinh\chi - \theta\chi). \tag{78}$$

The expressions of the parameters $\varphi_k, \theta, g'_k, \chi, C_0$, are defined in the Appendix.

The spin-boson interaction disappears at the zero-order approximation, Eq. (76), in the transformed Hamiltonian H' and the renormalized transition amplitude is $\Omega_r = \theta\Omega$. The delocalized phase regime [61] refers to nonvanishing values of the parameter θ. The first-order perturbation terms are collected in H'_1, Eq. (77), while the second- and higher-order perturbation terms appear in H'_2, Eq. (78). The contribution of the term H'_2 to the open dynamics can be neglected in the weak-coupling limit at zero temperature [60] and the transformed Hamiltonian is well approximated by the following form:

$$H_{\mathrm{eff}} = \frac{\theta\Omega}{2}\sigma_z + \sum_k g'_k\left(\sigma_-\otimes b_k^\dagger + \sigma_+\otimes b_k\right) + \sum_k \omega_k b_k^\dagger b_k + C_0. \tag{79}$$

The Hamiltonian (79) is evidently similar to the Hamiltonian (72) and is suitable for the analysis of the dynamics of the spin-boson model when the rotating-wave approximation is relaxed. The initial condition in the transformed frame is $|+\rangle_x\otimes|0\rangle_B$ and the polarization results in $P_z(t) = 2^{1/2}\mathrm{Re}\{h(t)\}$, where the function $h(t)$ is solution of the convoluted structure equation,

$$\dot{h}(t) + \imath\theta\Omega h(t) + \int_0^t f_r(t-t')h(t')dt' = 0, \tag{80}$$

with the initial condition $h(0) = 2^{-1/2}$. The function f_r is the transformed correlation function of the reservoir,

$$f_r(\tau) = \int_0^\infty J_r(\omega)e^{-\imath\omega\tau}d\omega,$$

and is defined in terms of the renormalized spectral density $J_r(\omega) = (4\pi)^{-1}\sum_k (g'_k)^2\delta(\omega-\omega_k)$. See Ref. [61] for details.

Similarly to the scenario found in the fermionic environment, the appearance of undamped oscillations in the polarization $P_z(t)$ depends on the critical value $\Omega^{(c)}$ of the transition amplitude. This value is defined in terms of the renormalized spectral density and the band-gap frequency Ω_g of the bosonic reservoir,

$$\Omega^{(c)} = \Omega_g + \int_{\Omega_g}^\infty \frac{J_r(\omega)}{\omega-\Omega_g}d\omega. \tag{81}$$

If the critical value $\Omega^{(c)}$ exceeds the value $\theta\Omega$ the polarization results in

$$P_z(t) = \mathrm{Re}\{e^{-\imath\Omega_g t}[\gamma_{\mathrm{sb}}e^{\imath\Delta_{\mathrm{sb}}\omega_s t} + I_{\mathrm{sb}}(\omega_s t)]\}, \quad \theta\Omega < \Omega^{(c)}. \tag{82}$$

The coefficients γ_{sb} and Δ_{sb} are defined in the Appendix in terms of the auxiliary function $\Lambda_r(\nu)$. Similarly to the previous cases, the auxiliary function $\Lambda_r(\nu)$ is defined in terms of the renormalized spectral density as $\Lambda_r(\nu) = J_r(\omega+\Omega_g)$ for every $\omega \geqslant 0$. The transient function $I_{\mathrm{sb}}(\omega_s t)$ is also defined in terms of the renormalized spectral density,

$$I_{\mathrm{sb}}(\omega_s t) = \int_{0^+}^\infty e^{-\imath\omega t}J_r(\omega+\Omega_g)/\big(\{\omega-\theta\Omega + \Omega_g + \mathcal{H}_+[J_r(\omega'+\Omega_g),\omega]\}^2 + \pi^2 J_r^2(\omega+\Omega_g)\big)d\omega, \tag{83}$$

and vanishes over long times. Consequently, undamped oscillations of the polarization appear for $t \gg 1/\omega_s$,

$$P_z(t) \sim \mathrm{Re}\{\gamma_{\mathrm{sb}}e^{\imath(\Delta_{\mathrm{sb}}\omega_s - \Omega_g)t}\}, \quad \theta\Omega < \Omega^{(c)}. \tag{84}$$

The frequency of the undamped oscillations is constant, $|\Delta_{\mathrm{sb}}\omega_s - \Omega_g|$, and vanishes for a special value of the band-gap frequency, $\Omega_g = \Delta_{\mathrm{sb}}\omega_s$. In this case the polarization persists for $t \gg 1/\omega_s$,

$$P_z(t) \sim \mathrm{Re}\{\gamma_{\mathrm{sb}}\}, \quad \theta\Omega < \Omega^{(c)}, \quad \Omega_g = \Delta_{\mathrm{sb}}\omega_s. \tag{85}$$

Again, the above analysis holds if the critical value of the transition amplitude is infinite, $\Omega^{(c)} = +\infty$.

If the critical value $\Omega^{(c)}$ is equal to the value $\theta\Omega$ the long-time behavior of the polarization depends on the structure of the renormalized spectral density at low frequencies, $J_r(\omega) \sim a_0(\omega-\Omega_g)^{\alpha_0}$ for $\omega \to \Omega_g^+$. For renormalized spectral densities that are superohmic in the band-gap frequency the polarization results in

$$P_z(t) = \gamma_{c,r}\cos(\Omega_g t) + \mathrm{Re}\{e^{-\imath\Omega_g t}I_{S,r}(\omega_s t)\}, \quad \theta\Omega = \Omega^{(c)}, \quad \alpha_0 > 1, \tag{86}$$

where the transient term $I_{S,r}(\omega_s t)$ reads

$$I_{S,r}(\omega_s t) = \int_{0^+}^{\infty} \frac{J_r(\omega+\Omega_g)e^{-\imath\omega t}}{\omega^2} \Bigg/ \Bigg[\frac{\pi^2 J_r^2(\omega+\Omega_g)}{\omega^2} + \left(1+\mathcal{H}_+\left[\frac{J_r(\omega'+\Omega_g)}{\omega'},\omega\right]\right)^2\Bigg] d\omega, \quad (87)$$

while the parameter $\gamma_{c,r}$ is defined in the Appendix. The transient term $I_{S,r}(\omega_s t)$ vanishes over long times and undamped oscillations of the polarizations appear for $t \gg 1/\omega_s$,

$$P_z(t) \sim \gamma_{c,r}\cos(\Omega_g t), \quad \theta\Omega = \Omega^{(c)}, \quad \alpha_0 > 1. \quad (88)$$

The oscillations disappear if the renormalized spectral density has no band gap,

$$P_z(t) \sim \gamma_{c,r}, \quad \theta\Omega = \Omega^{(c)}, \quad \alpha_0 > 1, \quad \Omega_g = 0. \quad (89)$$

If the critical value $\Omega^{(c)}$ equals the value $\theta\Omega$ and the renormalized spectral density is subohmic in the band-gap frequency the polarization results in

$$P_z(t) = e^{-\imath\Omega_g t} I_{\rm sb}(\omega_s t), \quad \theta\Omega = \Omega^{(c)}, \quad 1 > \alpha_0 > 0.$$

and vanishes over long times, $t \gg 1/\omega_s$. If the value $\theta\Omega$ exceeds the critical value $\Omega^{(c)}$ the polarization reads

$$P_z(t) = {\rm Re}\{e^{-\imath\Omega_g t} I_{\rm sb}(\omega_s t)\}, \quad (90)$$

and vanishes over long times.

Starting from the renormalized transition energy $\theta\Omega$ and the renormalized spectral density $J_r(\omega)$, a "dressed" energy $\epsilon_d^{(\rm sb)}$ can be defined

$$\epsilon_d^{(\rm sb)} = \theta\Omega - \int_{\Omega_g}^{\infty} \frac{J_r(\omega)}{\omega-\Omega_g}\, d\omega. \quad (91)$$

Over long times coherence persists in the two-level system if the dressed energy is below the band-gap energy, $\epsilon_d^{(\rm sb)} < \Omega_g$, and is entirely lost if the dressed energy exceeds the band-gap energy, $\epsilon_d^{(\rm sb)} > \Omega_g$. If the dressed energy equals the band-gap energy, $\epsilon_d^{(\rm sb)} = \Omega_g$, the loss of coherence is determined by the structure of the renormalized spectral density in the band-gap frequency. Again, coherence is completely lost in the subohmic regime and persists over long times if the renormalized spectral density is superohmic in the band-gap frequency.

If the renormalized spectral density belongs to the general class defined in Sec. IV the open dynamics exhibits inverse power-law relaxations to the asymptotic configurations. In fact, the transient terms exhibit oscillations enveloped in inverse power-law profiles. The power laws are arbitrarily faster than $1/(\omega_s t)$ for $\theta\Omega \neq \Omega^{(c)}$,

$$P_z(t) \sim {\rm Re}\{\gamma_{\rm sb} e^{\imath(\Delta_{\rm sb}\omega_s - \Omega_g)t}\} - |\eta_{\rm sb}|(\omega_s t)^{-1-\alpha_0} \times \sin(\Omega_g t + \pi\alpha_0/2), \quad \theta\Omega < \Omega^{(c)}, \quad (92)$$

$$P_z(t) \sim -|\eta_{\rm sb}|(\omega_s t)^{-1-\alpha_0}\sin(\Omega_g t + \pi\alpha_0/2), \quad \theta\Omega > \Omega^{(c)}, \quad (93)$$

and arbitrarily slow for $\theta\Omega = \Omega^{(c)}$,

$$P_z(t) \sim \gamma_c\cos(\Omega_g t) + |\eta_{c,r}|(\omega_s t)^{1-\alpha_0}\sin(\Omega_g t + \pi\alpha_0/2), \quad \theta\Omega = \Omega^{(c)}, \quad \alpha_0 > 1, \quad (94)$$

$$P_z(t) \sim -|\eta_s|(\omega_s t)^{\alpha_0-1}\sin(\Omega_g t - \pi\alpha_0/2), \quad \theta\Omega = \Omega^{(c)}, \quad 1 > \alpha_0 > 0. \quad (95)$$

The coefficients $\eta_{\rm sb}$, $\eta_{c,r}$, are defined in the Appendix. The present analysis of the conditions inducing undamped oscillation or persistence of the polarization improves the study performed in Ref. [63].

VII. CONCLUSIONS

We have considered a two-state nanoelectronic system that interacts with a fermionic environment. Coherence is maintained in the nanodevice by simple conditions that involve the corresponding degenerate energy level and a critical energy. This energy is defined via integral properties of the spectral density of the fermionic reservoir. If the degenerate energy level is less than or, in the superohmic regime, equal to the critical energy of the open system, undamped oscillation or persistence of coherence between the two states is maintained over long times for every initial coherent configuration of the nanosystem. Additional conditions induce coherence to approach asymptotically the initial value. The appearance of the oscillating or stable asymptotic nonvanishing regime depends on the value of the band-gap frequency of the reservoir. Furthermore, a dressed energy of the nanosystem can be defined such that coherence is maintained uniquely if the dressed energy is less than or, in the superohmic regime, equal to the band-gap energy of the reservoir. The behaviors of coherence reported above are found also in a nanocavity that is embedded in photonic crystals and, more generally, in a bosonic system with one single-particle energy level that interacts with a bosonic environment or in a two-level system that is coupled to a bosonic environment.

Following Ref. [38], the present model of a nanodevice interacting with a fermionic environment refers to a double quantum dot that is coupled to electrodes. Each dot has a single active energy level and all the spins are polarized both in the dots and electrodes. Alternatively, the model mimics a single-level quantum dot that is coupled to electrodes with possible spin-flip configurations in opposite directions. Single and double quantum dots are realized via semiconducting nanowires with tunable couplings [64]. The energy and decoherence of a pseudospin qubit in a semiconductor double quantum dot can be manipulated via a high-speed voltage pulse [65]. The description of an experimental apparatus that might detect the coherent behavior described above is out of the purposes of the present paper. Still, the critical energy that causes the transition from full decoherence to undamped oscillations or persistence of coherence might be observed in a nanosystem with a tunable degenerate energy level that is coupled to an electron reservoir.

ACKNOWLEDGMENT

The author thankfully acknowledges the anonymous referee for the fruitful suggestions on the dressed frequency.

APPENDIX: DETAILS

The study of the evolution of the coherence term $\rho_{+,-}(t)$ is performed via Eq. (20), where the function $u(t)$ is obtained by

solving Eq. (14). It is convenient to analyze the function $v(t)$, defined as $v(t) = \exp\{\imath\Omega_g t\}u(t)$, and its Laplace transform, $\tilde{v}(s) = \int_0^\infty \exp\{-st\}\, v(t)dt$. The equality $v(t) = \omega_s k(\omega_s t)$ defines the function $k(\xi)$ and its Laplace transform reads

$$\tilde{k}(\zeta) = \{\imath(E_0 - \Omega_g) + \omega_s\zeta - \imath\mathcal{S}[\Lambda(\nu), -\imath\zeta]\}^{-1}. \quad \text{(A1)}$$

The symbol $\mathcal{S}$ represents the Stieltjes transform [66–68], $\mathcal{S}[\Lambda(\nu), z] = \int_0^\infty \Lambda(\nu)/(\nu + z)\, d\nu$ for $|\arg z| < \pi$. The singularities of the function $\tilde{k}(\zeta)$ are determined by solving the following equation:

$$(E_0 - \Omega_g) - \imath\omega_s\zeta - \mathcal{S}[\Lambda(\nu), -\imath\zeta] = 0. \quad \text{(A2)}$$

The transcendental equation (A2) has been studied in Ref. [69]. The existence of the solution depends on the critical value E_c, given by Eq. (24), of the degenerate energy level E_0. This solution is imaginary, $\zeta = \imath\Delta$ with $\Delta > 0$, and exists uniquely for $E_0 < E_c$. Consequently, the complex valued function $\tilde{k}(\zeta)$ is well defined in the complex plane cut along the negative imaginary axis, $\zeta \neq \imath y$ for every $y \leqslant 0$, and exhibits uniquely one singularity, $\zeta = \imath\Delta$, for $E_0 < E_c$. This singularity contributes to the Laplace inversion via the corresponding residue,

$$\gamma = \omega_s \mathrm{Res}[\tilde{k}(\zeta), \imath\Delta], \quad E_0 < E_c. \quad \text{(A3)}$$

The function $k(\xi)$ is evaluated via the Laplace inversion of the function $\tilde{k}(\zeta)$,

$$k(\xi) = \lim_{y_0 \to +\infty} \frac{1}{2\pi\imath} \int_{x_0 - \imath y_0}^{x_0 + \imath y_0} e^{\xi\zeta}\tilde{k}(\zeta)d\zeta, \quad \text{(A4)}$$

where x_0 and y_0 are positive parameters. The above integration is performed via the corresponding line integral over the path $QABCDEFP$ in the complex plane, where $Q = x_0 - \imath y_0$, $A = \epsilon - \imath y_0$, $B = \epsilon(1 - \imath)$, $C = -\epsilon(1 + \imath)$, $D = -(\epsilon + \imath y_0)$, $E = \imath R$, $F = \imath y_0$, $P = x_0 + \imath y_0$, and $R = (\epsilon^2 + y_0^2)^{1/2}$. The counterclockwise circular arc BC is centered in the origin with radius $r = 2^{1/2}\epsilon$. The clockwise circular arc DE is centered in the origin with radius $R = (y_0^2 + \epsilon^2)^{1/2}$, respectively. The remaining paths are segments. For $y_0 \to +\infty$ and $\epsilon \to 0^+$ the contributions of paths QA, DE, EF, FP, vanish. If $E_0 \neq E_c$, or if $E_0 = E_c$ and $1 > \alpha_0 > 0$, the contribution of the path $ABCD$ in the limits $\epsilon \to 0^+$ and $y_0 \to +\infty$ is the following integral:

$$I_{ABCD}(\xi) = \int_{0^+}^{\infty} e^{-\imath\xi\nu}\Lambda(\nu)/(\{\mathcal{H}_+[\Lambda(\nu'), \nu] + \omega_s\nu - E_0 + \Omega_g\}^2 + \pi^2\Lambda^2(\nu))d\nu, \quad \text{(A5)}$$

and results in Eq. (26) by considering the definition of the auxiliary function $\Lambda(\nu)$ reported in Sec. III. No singularity of the function $\tilde{k}(\zeta)$ exists inside or belongs to the closed contour of integration $QABCDEFP$ if $E_0 \geqslant E_c$. One singularity appears inside the closed contour for $E_0 < E_c$ and contributes to the integration via the residue. This approach leads to Eqs. (25), (34), (35).

The integral (A5) vanishes for $\xi \gg 1$ and Eqs. (27) and (28) are found. The residue provides the undamped oscillations of Eqs. (25) and (27) and the persistent nonvanishing asymptotic behavior of Eq. (28). For the class of spectral densities introduced in Sec. IV, the integral $I_{ABCD}(\xi)$ decays according to inverse power laws [67] and leads to Eqs. (40), (42), (43), where

$$\eta = \frac{\omega_s a_0 \Gamma(1 + \alpha_0)}{(E_0 - E_c)^2} e^{-\imath\pi(1+\alpha_0)/2},$$

$$\eta_s = \frac{\omega_s \sin(\pi\alpha_0)}{\pi a_0 \Gamma(\alpha_0)} e^{\imath\pi(\alpha_0 - 1)/2}.$$

If $E_0 = E_c$ and $\alpha_0 > 1$ the following form,

$$\tilde{k}(\zeta) = \frac{1}{\omega_s + \mu_2}\left[\frac{1}{\zeta} - \frac{\imath\mathcal{S}[\Lambda(\nu)/\nu^2, -\imath\zeta]}{\omega_s + \mu_2} \Big/ \left(1 + \frac{\imath\zeta\mathcal{S}[\Lambda(\nu)/\nu^2, -\imath\zeta]}{\omega_s + \mu_2}\right)\right], \quad \text{(A6)}$$

gives the Laplace inversion

$$k(\xi) = \frac{\gamma_c}{\omega_s}\left\{1 + \frac{\gamma_c}{\omega_s}\int_{0^+}^{\infty} e^{-\imath\xi\nu}\frac{\Lambda(\nu)}{\nu^2} \Big/ \left[\left(1 + \frac{\gamma_c}{\omega_s}\nu\,\mathcal{H}_+\left[\frac{\Lambda(\nu')}{(\nu')^2}, \nu\right]\right)^2 + \pi^2\left(\frac{\gamma_c}{\omega_s}\right)^2\frac{\Lambda^2(\nu)}{\nu^2}\right]d\nu\right\}. \quad \text{(A7)}$$

The parameter γ_c is defined as $\gamma_c = \omega_s/(\omega_s + \mu_2)$, where $\mu_2 = \int_0^\infty \Lambda(\nu)/\nu^2 d\nu$, and results in the expression (30). In this way, Eqs. (29) and (31) are found. Notice that the integral that defines the constant μ_2 exists finite due to the superohmic behavior of the spectral density. The integral appearing on the right-hand side of Eq. (A7) vanishes for $\xi \gg 1$. In this way we find Eqs. (32) and (33). For the class of auxiliary functions $\Lambda(\nu)$ introduced in Sec. IV, the integral appearing on the right-hand side of Eq. (A7) exhibits inverse power-law decays [67] as $\xi \gg 1$ and Eq. (41) is found, where

$$\eta_c = \frac{\gamma_c^2 a_0 \Gamma(\alpha_0 - 1) e^{\imath\pi(1-\alpha_0)/2}}{\omega_s}.$$

In Sec. V the special spectral densities (44) and (45) correspond to auxiliary functions $\Lambda_1(\nu)$ and $\Lambda_2(\nu)$ that are defined by the following forms:

$$\Lambda_1(\nu) = \frac{j_1\nu^\alpha}{\nu^2 + \lambda^2}, \quad 1 > \alpha > 0, \quad \text{(A8)}$$

$$\Lambda_2(\nu) = \frac{j_2\nu^\beta}{(\nu + l)(\nu^2 + \lambda^2)}, \quad 2 > \beta > 0, \quad \text{(A9)}$$

where $\lambda, l > 0$. The corresponding forms of the function $\tilde{k}(\zeta)$ are

$$\tilde{k}_1(\zeta) = \frac{(\zeta^2 - \lambda^2)/\omega_s}{\zeta^3 + \imath r_2\zeta^2 + r_1\zeta + r_\alpha e^{-\imath\pi(1+\alpha)/2}\zeta^\alpha + \imath r_0},$$

$$\tilde{k}_2(\zeta) = \frac{(\zeta^3 - \imath l\zeta^2 - \lambda^2\zeta + \imath l\lambda^2)/\omega_s}{\zeta^4 + \imath q_3\zeta^3 + q_2\zeta^2 - q_\beta e^{-\imath\pi\beta/2}\zeta^\beta + \imath q_1\zeta + q_0},$$

where

$$r_0 = \frac{1}{\omega_s}\left(\frac{\pi j_1 \lambda^\alpha \csc(\pi\alpha/2)}{2} + \lambda^2(\Omega_g - E_0)\right),$$

$$r_\alpha = \frac{\pi j_1 \csc(\pi\alpha)}{\omega_s}, \quad r_2 = \frac{E_0 - \Omega_g}{\omega_s},$$

$$r_1 = \frac{\pi j_1 \lambda^{\alpha-1} \sec(\pi\alpha/2)}{2\omega_s} - \lambda^2,$$

and

$$\begin{aligned} q_0 &= \{\pi j_2[2l^\beta\lambda^2 \csc(\pi\beta) - l\lambda^{1+\beta}\sec(\pi\beta/2) \\ &\quad + l^2\lambda^\beta \csc(\pi\beta/2)]/[2(l^2+\lambda^2)] \\ &\quad + l\lambda^2(\Omega_g - E_0)\}/\omega_s, \\ q_1 &= [\lambda^2(\Omega_g - E_0) - \pi j_2 \lambda^{\beta-1}\sec(\pi\beta/2)/2]/\omega_s \\ &\quad + l\lambda^2, \quad q_\beta = \pi j_2 \csc(\pi\beta)/\omega_s, \\ q_2 &= \{\pi j_2[\lambda^\beta \csc(\pi\beta/2)/2 + l\lambda^{\beta-1}\sec(\pi\beta/2)/2 \\ &\quad - l^\beta \csc(\pi\beta)]/(l^2+\lambda^2) + l(E_0 - \Omega_g)\}/\omega_s - \lambda^2, \\ q_3 &= -l + (E_0 - \Omega_g)/\omega_s. \end{aligned}$$

The term by term Laplace inversion [70] of the series expansions of the functions $\tilde{k}_1(\zeta)$ and $\tilde{k}_2(\zeta)$ for large ζ leads to Eqs. (46) and (47), where

$$C^{(>1)}_{n,k,j} = \frac{(-1)^n r_1^{n-k} r_0^{k-j} r_\alpha^j e^{\imath\pi(k-2j-\alpha j)/2}}{j!(n-k)!(k-j)!},$$

$$C^{(2)}_{n,k,j,m} = \frac{(-1)^{n+m} q_2^{n-k} q_1^{k-j} q_0^{j-m} q_\beta^m e^{\imath\pi(k-j-\beta m)/2}}{m!(n-k)!(k-j)!(j-m)!}.$$

For rational values p/q of the powers α and β, the functions $k_1(\xi)$ and $k_2(\xi)$ are obtained as the Laplace inversions of the rational functions $K_1(w)$ and $K_2(w)$,

$$\begin{aligned} K_1(w) &= [(w^{2q} - \lambda^2)/\omega_s]/(w^{3q} + \imath r_2 w^{2q} + r_1 w^q \\ &\quad + r_\alpha e^{-\imath\pi(1+\alpha)/2} w^p + \imath r_0), \\ K_2(w) &= [(w^{3q} - \imath l w^{2q} - \lambda^2 w^q + \imath l\lambda^2)/\omega_s]/(w^{4q} \\ &\quad + \imath q_3 w^{3q} + q_2 w^{2q} - q_\beta e^{-\imath\pi\beta/2} w^p + \imath q_1 w^q + q_0), \end{aligned}$$

where $w = \zeta^{1/q}$. Let the roots of the denominators of the rational function $K_j(w)$ be $\sigma_1^{(j)}, \ldots, \sigma_{n_j}^{(j)}$, with multiplicity $m_1^{(j)}, \ldots, m_{n_j}^{(j)}$, for every $j = 1,2$. The Laplace inversion of the decomposition of the rational functions leads to Eq. (50), where

$$\Phi^{(j)}_{l,k} = \frac{1}{(k-1)!\left(m_l^{(j)} - k\right)!} \frac{d^{k-1}}{dw^{k-1}} \times \left[\left(w - \sigma_l^{(1)}\right)^{m_l} K_j(w)\right]_{w=\sigma_l^{(j)}}, \tag{A10}$$

for every $l = 1, \ldots, n_j$, $k = 1, \ldots, m_l^{(j)}$, and $j = 1,2$.

The study of coherence of a qubit interacting with a bosonic environment is performed by solving Eq. (57). The functions $v_b(t)$ and $k_b(t)$ are defined as follows: $v_b(t) = e^{\imath(\Omega_g - \omega_0)t} G(t)$ and $\tilde{v}_b(t) = \tilde{k}_b(s/\omega_s)$. The latter Laplace transform reads

$$\tilde{k}_b(\zeta) = \{\imath(\omega_0 - \Omega_g) + \omega_s\zeta - \imath\mathcal{S}[\Lambda(\nu), -\imath\zeta]\}^{-1}, \tag{A11}$$

and is analyzed with the approach reported above. In this way, Eqs. (58)–(70) are obtained, where

$$\gamma_b = \omega_s \mathrm{Res}[\tilde{k}_b(\zeta), \imath\Delta_b], \quad \omega_0 < \omega_c, \tag{A12}$$

and

$$\eta_b = \frac{\omega_s a_0 \Gamma(1+\alpha_0)}{(\omega_0 - \omega_c)^2} e^{-\imath\pi(1+\alpha_0)/2}.$$

The polarization of the delocalized phase regime of the spin-boson model is studied by solving Eq. (80). The functions $v_{\mathrm{sb}}(t)$ and $k_{\mathrm{sb}}(t)$ are defined as follows: $v_{\mathrm{sb}}(t) = e^{\imath\Omega_g t} h(t)$ and $\tilde{v}_{\mathrm{sb}}(t) = \tilde{k}_{\mathrm{sb}}(s/\omega_s)$. The latter Laplace transform results in

$$\tilde{k}_{\mathrm{sb}}(\zeta) = h(0)\{\imath(\theta\Omega - \Omega_g) - \imath\mathcal{S}[\Lambda(\nu), -\imath\zeta] \quad + \omega_s\zeta\}^{-1}, \tag{A13}$$

and is analyzed with the approach reported above. The involved parameters are

$$\theta = \exp\left\{-\sum_k \frac{g_{b,k}^2 \varphi_k^2}{2\omega_k^2}\right\}, \quad g'_k = \frac{\theta\Omega g_{b,k}\varphi_k}{\omega_k},$$

$$C_0 = \sum_k \frac{g_{b,k}^2 \varphi_k}{4\omega_k}(\varphi_k - 2), \quad \chi = \sum_k \frac{g_{b,k}\varphi_k}{\omega_k}(b_k^\dagger - b_k).$$

See Ref. [61] for details. In this way we find Eqs. (81)–(95), where

$$\gamma_{\mathrm{sb}} = \omega_s \mathrm{Res}[\tilde{k}_{\mathrm{sb}}(\zeta), \imath\Delta_{\mathrm{sb}}], \quad \theta\Omega < \Omega^{(c)}, \tag{A14}$$

and

$$\eta_{\mathrm{sb}} = \frac{\omega_s a_0 \Gamma(1+\alpha_0)}{(\theta\Omega - \Omega^{(c)})^2} e^{-\imath\pi(1+\alpha_0)/2},$$

$$\gamma_{c,r} = \frac{\omega_s}{\omega_s + \int_0^\infty \Lambda_r(\nu)/\nu^2 d\nu}.$$

This concludes the demonstrations of the results reported in the paper.

[1] L. Fedichkin and V. Privman, in *Electron Spin Resonance and Related Phenomena in Low-Dimensional Structures* (Springer, Berlin, 2009), pp. 141–167.

[2] H. P. Breuer and F. Petruccione, *The Theory of Open Quantum Systems* (Oxford University Press, Oxford, 2002).

[3] U. Weiss, *Quantum Dissipative Systems*, 3rd ed. (World Scientific, Singapore, 2008).

[4] M. A. Nielsen and I. L. Chuang, *Quantum Computation and Quantum Information* (Cambridge University Press, Cambridge, England, 2000).

[5] D. P. Di Vincenzo, Science **270**, 255 (1995); W. G. Unruh, Phys. Rev. A **51**, 992 (1995); P. W. Shor, W. H. Zurek, I. L. Chuang, and R. Laflamme, Science **270**, 1633 (1995).

[6] W. H. Zurek, Phys. Rev. D **26**, 1862 (1982).

[7] P. Zanardi and M. Rasetti, Phys. Rev. Lett. **79**, 3306 (1997); Mod. Phys. Lett. B **11**, 1085 (1997).

[8] D. A. Lidar, I. L. Chuang, and K. B. Whaley, Phys. Rev. Lett. **81**, 2594 (1998); P. Zanardi, Phys. Rev. A **57**, 3276 (1998).

[9] R. I. Karasik, K.-P. Marzlin, B. C. Sanders, and K. B. Whaley, Phys. Rev. A **77**, 052301 (2008).

[10] D. Bacon, D. A. Lidar, and K. B. Whaley, Phys. Rev. A **60**, 1944 (1999); A. Shabani and D. A. Lidar, *ibid.* **72**, 042303 (2005).

[11] D. A. Pushin, M. G. Huber, M. Arif, and D. G. Cory, Phys. Rev. Lett. **107**, 150401 (2011).

[12] D. Wei, J. Luo, X. Sun, X. Zeng, M. Zhan, and M. Liu, Phys. Rev. Lett. **95**, 020501 (2005).

[13] C. Langer, R. Ozeri, J. D. Jost, J. Chiaverini, B. DeMarco, A. Ben-Kish, R. B. Blakestad, J. Britton, D. B. Hume, W. M. Itano, D. Leibfried, R. Reichle, T. Rosenband, T. Schaetz, P. O. Schmidt, and D. J. Wineland, Phys. Rev. Lett. **95**, 060502 (2005).

[14] T. Yamamoto, K. Hayashi, A. K. Özdemir, M. Koashi, and N. Imoto, Nat. Photon. **2**, 488 (2008).

[15] F. O. Prado, E. I. Duzzioni, M. H. Y. Moussa, N. G. de Almeida, and C. J. Villas-Bôas, Phys. Rev. Lett. **102**, 073008 (2009); K. W. Murch, U. Vool, D. Zhou, S. J. Weber, S. M. Girvin, and I. Siddiqi, *ibid.* **109**, 183602 (2012); A. Sarlette, J. M. Raimond, M. Brune, and P. Rouchon, *ibid.* **107**, 010402 (2011); S. L. Wu, L. C. Wang, and X. X. Yi, J. Phys. A **45**, 405305 (2012); S. L. Wu, Phys. Rev. A **91**, 032104 (2015).

[16] D. Chruscinski and A. Kossakowski, J. Phys. B **45**, 154002 (2012).

[17] A. Rivas, S. F. Huelga, and M. B. Plenio, Rep. Prog. Phys. **77**, 094001 (2014).

[18] A. Kossakowski, Rep. Math. Phys. **3**, 247 (1972); Bull. Acad. Polon. Sci. Ser. Math. Astr. Phys. **20**, 1021 (1972); **21**, 649 (1973).

[19] V. Gorini, A. Kossakowski, and E. C. G. Sudarshan, J. Math. Phys. **17**, 821 (1976).

[20] G. Lindblad, Commun. Math. Phys. **48**, 119 (1976).

[21] A. Beige, D. Braun, B. Tregenna, and P. L. Knight, Phys. Rev. Lett. **85**, 1762 (2000); W. T. Strunz, F. Haake, and D. Braun, Phys. Rev. A **67**, 022101 (2003); O. Oreshkov and J. Calsamiglia, Phys. Rev. Lett. **105**, 050503 (2010).

[22] W.-M. Zhang, P.-Y. Lo, H.-N. Xiong, M. W.-Y. Tu, and F. Nori, Phys. Rev. Lett. **109**, 170402 (2012).

[23] P. Zanardi and L. C. Venuti, Phys. Rev. Lett. **113**, 240406 (2014).

[24] M. Chen and J. Q. You, Phys. Rev. A **87**, 052108 (2013).

[25] M. W. Y. Tu and W. M. Zhang, Phys. Rev. B **78**, 235311 (2008).

[26] M. W. Y. Tu, M. T. Lee, and W. M. Zhang, Quantum Inf. Process. **8**, 631 (2009).

[27] H. N. Xiong, W. M. Zhang, X. Wang, and M. H. Wu, Phys. Rev. A **82**, 012105 (2010).

[28] J. Jin, M. W. Y. Tu, W. M. Zhang, and Y. Yan, New J. Phys. **12**, 083013 (2010).

[29] M. H. Wu, C. U. Lei, W. M. Zhang, and H. N. Xiong, Opt. Express **18**, 18407 (2010).

[30] H. T. Tan and W. M. Zhang, Phys. Rev. A **83**, 032102 (2011).

[31] C. U. Lei and W. M. Zhang, Phys. Rev. A **84**, 052116 (2011).

[32] C. U. Lei and W. M. Zhang, Ann. Phys. (NY) **327**, 1408 (2012).

[33] M. W.-Y. Tu, J.-H. Liu, and W.-M. Zhang, arXiv:1503.05376v1.

[34] A. Ferraz and E. Kochetov, Eur. Phys. J. B **86**, 512 (2013).

[35] X. S. Ma, A. M. Wang, X. D. Yang, and H. You, J. Phys. A **38**, 2761 (2005).

[36] Y. Y. Chen, X. L. Feng, and C. H. Oh, Quantum Inf. Process. **13**, 547 (2014); G. Xu and G. Long, Sci. Rep. **4**, 6814 (2014).

[37] J. Schwinger, J. Math. Phys. **2**, 407 (1961); L. V. Keldysh, Sov. Phys. JETP **20**, 1018 (1965).

[38] H.-N. Xiong, W.-M. Zhang, M. W.-Y. Tu, and D. Braun, Phys. Rev. A **86**, 032107 (2012).

[39] E. C. Titchmarsh, *The Theory of Functions*, 2nd ed. (Oxford University Press, London, 1939).

[40] M. Woldeyohannes and S. John, J. Opt. B **5**, R43 (2003); Phys. Rev. A **60**, 5046 (1999).

[41] T. Quang, M. Woldeyohannes, S. John, and G. S. Agarwal, Phys. Rev. Lett. **79**, 5238 (1997); S. John and T. Quang, Phys. Rev. A **50**, 1764 (1994); Phys. Rev. Lett. **74**, 3419 (1995); **78**, 1888 (1997).

[42] F. Giraldi and F. Petruccione, J. Phys. A **47**, 395304 (2014).

[43] F. Giraldi and F. Petruccione, J. Phys. B **48**, 035202 (2015).

[44] A. M. Mathai, R. K. Saxena, and H. J. Haubold, *The H-Function: Theory and Applications* (Springer-Verlag, New York, 2010).

[45] R. P. Feynman and F. L. Vernon, Ann. Phys. **24**, 118 (1963); B. L. Hu, J. P. Paz, and Y. H. Zhang, Phys. Rev. D **45**, 2843 (1992).

[46] E. T. Jaynes and F. W. Cummings, Proc. IEEE **51**, 89 (1963).

[47] B. M. Garraway, Phys. Rev. A **55**, 2290 (1997); **55**, 4636 (1997); B. J. Dalton, S. M. Barnett, and B. M. Garraway, *ibid.* **64**, 053813 (2001); I. E. Linington and B. M. Garraway, J. Phys. B **39**, 3383 (2006); Phys. Rev. A **77**, 033831 (2008).

[48] B. Vacchini and H. P. Breuer, Phys. Rev. A **81**, 042103 (2010).

[49] F. Giraldi and F. Petruccione, Phys. Rev. A **85**, 062107 (2012).

[50] A. J. Leggett, S. Chakravarty, A. T. Dorsey, M. P. A. Fisher, A. Garg, and W. Zwerger, Rev. Mod. Phys. **59**, 1 (1987).

[51] S. K. Kehrein and A. Mielke, Phys. Lett. A **219**, 313 (1996); R. Bulla, N.-H. Tong, and M. Vojta, Phys. Rev. Lett. **91**, 170601 (2003); D. P. DiVincenzo and D. Loss, Phys. Rev. B **71**, 035318 (2005); M. Vojta, R. Bulla, F. Güttge, and F. Anders, *ibid.* **81**, 075122 (2010); M. Vojta, *ibid.* **85**, 115113 (2012); A. Winter, H. Rieger, M. Vojta, and R. Bulla, Phys. Rev. Lett. **102**, 030601 (2009); A. Alvermann and H. Fehske, *ibid.* **102**, 150601 (2009); M. Thorwart, E. Paladino, and M. Grifoni, Chem. Phys. **296**, 333 (2004); Y. Y. Zhang, Q. H. Chen, and K. L. Wang, Phys. Rev. B **81**, 121105(R) (2010).

[52] V. M. Kenkre and L. Giuggioli, Chem. Phys. **296**, 135 (2004); L. Bonci, P. Grigolini, R. Roncaglia, and D. Vitali, Phys. Rev. A **47**, 3538 (1993).

[53] D. Braak, Ann. Phys. **525**, L23 (2013); J. Phys. A **46**, 175301 (2013); Phys. Rev. Lett. **107**, 100401 (2011); H. Dekker, Phys. Rev. A **35**, 1436 (1987).

[54] A. Chin and M. Turlakov, Phys. Rev. B **73**, 075311 (2006).

[55] F. B. Anders, R. Bulla, and M. Vojta, Phys. Rev. Lett **98**, 210402 (2007); R. Bulla, T. A. Costi, and T. Pruschke, Rev. Mod. Phys. **80**, 395 (2008); A. W. Chin, J. Prior, S. F. Huelga, and M. B. Plenio, Phys. Rev. Lett. **107**, 160601 (2011); M. Vojta, N. H. Tong, and R. Bulla, *ibid.* **94**, 070604 (2005).

[56] A. G. Kofman, G. Kurizki, and B. Sherman, J. Mod. Opt. **41**, 353 (1994); A. G. Kofman and G. Kurizki, Phys. Rev. Lett. **93**, 130406 (2004); G. Gordon, G. Kurizki, and D. A. Lidar, *ibid.* **101**, 010403 (2008); A. G. Kofman and G. Kurizki, Nature (London) **405**, 546 (2000); Phys. Rev. Lett. **87**, 270405 (2001).

[57] J. Prior, A. W. Chin, A. Rivas, S. F. Huelga, and M. B. Plenio, Phys. Rev. Lett. **105**, 050404 (2010); A. W. Chin, S. F. Huelga, and M. B. Plenio, J. Math. Phys. **51**, 092109 (2013).
[58] Q. J. Tong, J. H. An, H. G. Luo, and C. H. Oh, Phys. Rev. B **84**, 174301 (2011).
[59] R. Silbey and R. A. Harris, J. Chem. Phys. **80**, 2615 (1984).
[60] H. Zheng, Eur. Phys. J. B **38**, 559 (2004); Z. Lu and H. Zheng, Phys. Rev. B **75**, 054302 (2007); A. W. Chin, *ibid.* **76**, 201307(R) (2007).
[61] H. B. Liu, J. H. An, C. Chen, Q. J. Tong, H. G. Luo, and C. H. Oh, Phys. Rev. A **87**, 052139 (2013).
[62] F. Giraldi and F. Petruccione, Phys. Rev A **88**, 042102 (2013).
[63] F. Giraldi and F. Petruccione, Eur. Phys. J. D **68**, 24 (2014).
[64] C. Fasth, A. Fuhrer, M. T. Bjork, and L. Samuelson, Nano Lett. **5**, 1487 (2005).
[65] T. Hayashi, T. Fujisawa, H. D. Cheong, Y. H. Jeong, and Y. Hirayama, Phys. Rev. Lett. **91**, 226804 (2003).
[66] D. V. Widder, *The Laplace Transform* (Princeton University Press, Princeton, NJ, 1941).
[67] R. Wong, *Asymptotic Approximations of Integrals* (Academic, Boston, 1989).
[68] R. Wong and Yu-Qiu Zhao, Proc. R. Soc. London, Ser. A **458**, 625 (2002).
[69] F. Giraldi, arXiv:1502.01551v1.
[70] F. Giraldi and F. Petruccione, J. Phys. A **45**, 285306 (2012).